

*Letter to the Editor***The frequency resolved spectroscopy of Cyg X-1:  
fast variability of the Fe  $K_{\alpha}$  line**M. Revnivtsev<sup>1,2</sup>, M. Gilfanov<sup>2,1</sup>, and E. Churazov<sup>2,1</sup><sup>1</sup> Space Research Institute, Russian Academy of Sciences, Profsoyuznaya 84/32, 117810 Moscow, Russia,<sup>2</sup> Max-Planck-Institute für Astrophysik, Karl-Schwarzschild-Strasse 1, D-85740 Garching bei München, Germany

Received 11 May 1999 / Accepted 11 June 1999

**Abstract.** We studied the frequency resolved energy spectra of Cyg X-1 during the standard low (hard) spectral state using the data of the Rossi X-Ray Timing Explorer. We found that the relative amplitude of the reflection features – the iron fluorescent line at  $\sim 6.5$  keV and the smeared edge above  $\sim 7$  keV – decreases with the increasing frequency. In particular we found that the equivalent width of the iron line decreases above  $\sim 1$  Hz and drops twice in value at a frequency of  $\sim 10$  Hz.

The assumption that such behavior is solely due to a finite light crossing time of the reflecting media, would imply the characteristic size of the reflector  $\sim 5 \times 10^8$  cm, corresponding to  $\sim 150R_g$  for a  $10M_{\odot}$  black hole. Alternatively the lack of high frequency oscillations of the reflected component may indicate that the short time scale,  $\sim 50$ – $100$  msec, variations of the primary continuum appear in the geometrically different, likely inner, part of the accretion flow and give a rise to a significantly weaker, if any, reflected emission than the longer time scale events.

**Key words:** methods: data analysis – stars: binaries: general – stars: individual: (Cyg X-1) – X-rays: general

**1. Introduction**

Over the last several years it has become widely accepted that the Galactic X-ray binaries exhibit Compton reflection features in their spectra.

Qualitatively, the reflection component in the X-ray spectra of these systems can be described as a broad “hump” at energies of 20–30 keV, a fluorescent Fe line at energies 6.4–6.7 keV (depending on the ionization state of the reflecting medium) and an absorption edge at the energy  $\approx 7.1$  keV (Basko et al., 1974, George & Fabian, 1991). For all geometries which do not obscure the direct primary continuum from the observer, the detected energy spectra consists of this direct component (approximately a power law in the 3–13 keV energy band) and the reflection features. For standard cosmic abundances the expected

equivalent width of the fluorescent Fe line is  $\sim 100$ – $200$  eV (for a source above semi-infinite slab of neutral matter).

The geometry and mutual location of the source of primary continuum and reflecting medium should affect both the equivalent width of the fluorescent line and the character of its variability. In particular the finite size of the reflector implies that the time variations of the reflected radiation should be smeared out on the time scales corresponding to the light crossing time of the reflector. In addition, time lags between different emission components might appear. Alternatively, the geometrically different region of the main energy release zone (where the primary continuum is produced) may have a different efficiency for the production of the reflection component. As a result the timing properties of the reprocessed component may be linked to the properties of the selected region of this zone.

**2. Observations and data analysis**

For our analysis we chose the publicly available data of the Rossi X-ray Timing Explorer observations P10238 performed between Mar. 26, 1996 and Mar. 31, 1996 with a total exposure time  $\sim 70$  ksec (we used only observations where all 5 PCU were turned on). For the frequency resolved spectral analysis we used the PCA data in the “Generic Binned” mode, having a  $\frac{1}{64}$  sec  $\sim 16$  msec time resolution in 64 energy channels covering the whole PCA energy band (B\_16ms\_64M\_0\_249). For an analysis of the averaged spectrum we used the “Standard Mode 2” data, which has twice as many energy channels in the energy band of our interest (3–13 keV) as the “Generic Binned” mode.

For the obtained spectra we constructed the response matrix using the standard tasks of the FTOOLS 4.2 package with PCA RMF v3.5 (Jahoda 1999). The comparison of the timing mode spectra with that obtained from the “Standard Mode 2” showed, that they do not differ by more than 1–1.5%. The background was calculated using the “Q6” model (VLE-based model, preferable for bright sources does not work for these observations). However, the PCA background is negligible for the time averaged spectra of Cyg X-1 in the energy band of 3–13 keV. The PCA background contribution to the frequency

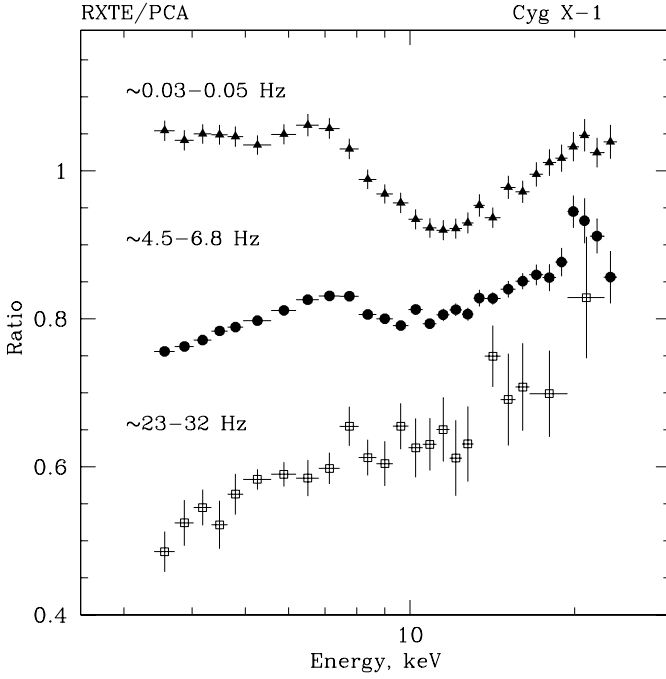


**Fig. 1.** The ratio of the energy spectra of Cyg X-1 in different frequency bands to a power law model with the photon index  $\alpha = 1.8$ . Spectra corresponding to 0.03–0.05 Hz and 23–32 Hz were rescaled for clarity.

resolved spectra at the frequencies 0.03–30 Hz is even less important.

### 3. Frequency resolved spectral analysis

We calculated the Power Density Spectra (PDSs) in each energy channel for every 128 sec time segments using the standard Fast Fourier Transform (FFT) procedure and adopting the normalization of Miyamoto et al. (1991):

$$P_j = 2|a_j|^2/N_\gamma R$$

$$a_j = \sum_{k=1}^{2^m} x_k e^{i\omega_j t_k}$$

where  $t_k$  is the time label of the  $k$ th bin,  $x_k$  is the number of counts in this bin,  $N_\gamma$  is the total number of photons and  $R$  is the average count rate in the segment ( $R = N_\gamma/T$ ,  $T$  – total duration of the light curve segment). This PDS normalization ( $(\text{rms}/\text{mean})^2/\text{Hz}$ ) allows one to obtain squared fractional  $\text{rms}$  by integrating the power over the frequencies of interest. Then the obtained power spectra were averaged over the light curve segments and the logarithmic frequency bins. For every obtained frequency bin the frequency dependent spectra were constructed according to the formula:

$$S(E_i, f_j) = R_i \sqrt{P_i(f_j) \Delta f_j} = \sqrt{\frac{2|a_{ij}|^2}{T}} \Delta f_j.$$

Here  $S(E_i, f_j)$  is the count rate of the spectrum on the frequency  $f_j$  in the energy channel  $E_i$ . Since the light curves of Cyg X-1

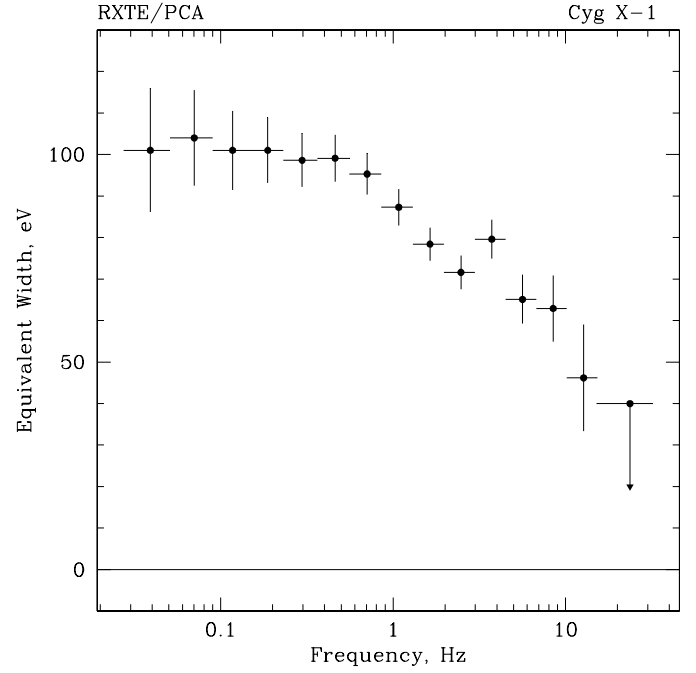


**Fig. 2.** Dependence of the equivalent width of the fluorescent Fe line on the frequency. For the spectral approximation the powerlaw+gaussian line model was used (3–13 keV energy band, the centroid energy and the width of the line were frozen at the values 6.4 keV and 0.1 keV respectively).

in the different energy bands are almost perfectly coherent and have practically the same form of the PDS (see e.g. Nowak et al. 1999), the spectra obtained using the procedure above can be used to describe the real energy spectrum of the source X-ray flux variations on the different time scales. The above expression can also be easily adapted to describe the energy spectrum of different PDS spectrum components.

### 4. Results

The energy spectra of Cyg X-1 in several narrow frequency ranges between 0.03 and 30 Hz are shown in Fig. 1. The change of the spectral shape with the decrease of the characteristic time scale can be clearly seen. The relative amplitude of the reflection features, in particular that of the broad line at  $\sim 6$ –7 keV and the “smeared edge” above  $\sim 7$  keV, is apparently decreasing with the increase of frequency and vanishes above  $\sim 20$  Hz. Along with becoming less “wiggled” the spectra become harder as frequency increases.

In order to quantify these effects we fit frequency resolved spectra in 16 frequency bins covering the 0.03–32 Hz range in the 3–13 keV energy band with a simple two component model consisting of a power law and a Gaussian line with the fixed energy  $E_{\text{line}} = 6.4$  keV and the width  $\text{FWHM} = 0.1$  keV (that is comparable with the PCA energy resolution at this energy). The best fit parameters are given in Table 1. The dependence of the line equivalent width upon frequency is shown in Fig. 2. As is seen from Fig. 2, the equivalent width of the line starts

**Table 1.** Best fit parameters of the approximation of frequency dependent spectra of Cyg X-1 with the power law + gaussian line (line energy and width were frozen at the values 6.4 keV and 0.1 keV respectively) in the energy band 3–13 keV.

Freq., Hz	PL slope, $\alpha$	EW, eV
$(3.9 \pm 1.2) \times 10^{-2}$	$1.93 \pm 0.01$	$101 \pm 15$
$(7.0 \pm 1.9) \times 10^{-2}$	$1.91 \pm 0.01$	$104 \pm 12$
$0.12 \pm 0.03$	$1.91 \pm 0.01$	$101 \pm 9$
$0.19 \pm 0.04$	$1.89 \pm 0.01$	$101 \pm 8$
$0.30 \pm 0.07$	$1.89 \pm 0.01$	$98.6 \pm 6.4$
$0.46 \pm 0.09$	$1.89 \pm 0.01$	$99.1 \pm 5.6$
$0.7 \pm 0.14$	$1.89 \pm 0.01$	$95.3 \pm 4.9$
$1.07 \pm 0.22$	$1.86 \pm 0.01$	$87.3 \pm 4.4$
$1.63 \pm 0.33$	$1.83 \pm 0.01$	$78.4 \pm 3.9$
$2.48 \pm 0.50$	$1.81 \pm 0.01$	$71.6 \pm 4.0$
$3.74 \pm 0.76$	$1.80 \pm 0.01$	$79.6 \pm 4.7$
$5.63 \pm 1.14$	$1.75 \pm 0.01$	$65.1 \pm 5.8$
$8.48 \pm 1.71$	$1.70 \pm 0.01$	$62.9 \pm 7.9$
$12.7 \pm 2.6$	$1.63 \pm 0.01$	$46.2 \pm 12.8$
$19.2 \pm 3.8$	$1.62 \pm 0.01$	$< 48^a$
$27.5 \pm 4.5$	$1.63 \pm 0.01$	$< 57^a$

<sup>a</sup>  $2\sigma$  upper limit

decreasing above  $\sim 1$  Hz and falls by a factor of 2 at  $\sim 10$  Hz. No significant flux in the line was detected above 15 Hz with a  $2\sigma$  upper limit on the equivalent width in the 15–32 Hz frequency range of  $\approx 40$  eV.

Variations of the parameters of the spectral model, in particular the change of the line centroid to 6.0 and 6.7 keV and the increase of the line width to 1.0 keV, do not change the general trend. These variations, however, affect the particular values of the equivalent width and, to some extent, the shape of the curve in Fig. 2. The change of the line centroid energy to the 5 keV or 9 keV, on the contrary, results in the disappearance of the effect.

Finally we should mention that similar behaviour of the frequency resolved spectra was detected in Cyg X-1 observations 20175-01-01-00, 20175-01-02-00 and in all available observations of the set P30157 (01–10), performed in 1997 but with lower significance.

## 5. Discussion

A time averaged energy spectrum of Cyg X-1 (e.g. Ebisawa et al. 1992, Gierlinski et al. 1997) as well as frequency resolved spectra at low frequency (Fig. 1) show a clear deviation from a single slope power law spectrum. This deviation is commonly ascribed to the reflection from an optically thick media located in the vicinity of the production site of primary hard X-ray radiation. In a simple case of reflection from an optically thick cold neutral medium the main reflection features are well known (Basko et al., 1974, George & Fabian, 1991) – a narrow unshifted iron  $K_\alpha$  line at 6.4 keV with an equivalent width of  $\sim 100$  eV, an absorption edge at  $\approx 7.1$  keV and a reflected continuum peaked at  $\sim 20$ – $30$  keV. However, the real spectra of compact X-ray binaries show considerably more compli-

cated behavior. In particular the centroid energy of the line is often different from 6.4 keV, the line width in many cases is as large as  $\sim 1$  keV and a broad “smeared edge” above  $\sim 7$ – $8$  keV is observed instead of a sharp absorption edge at  $\approx 7.1$  keV (Ebisawa et al. 1992). This departure from a simple reflection model hints at a complicated ionization state and/or motion (e.g. Keplerian motion in the disk) of the reflecting media.

It is obvious, that the simple spectral model used for fitting the data in the previous section is neither adequate nor completely justified from the physical point of view. The apparent line centroid energy and width vary with frequency. In particular the best fit centroid energy shifts below 6.0 keV and the width of the line exceeds 1 keV as the frequency increases. However, due to the lack of a satisfactory realistic model of reflection in an X-ray binary, especially applicable to the frequency resolved spectral data, we restricted ourselves to the simple two component model described in the previous section. The main purpose of using this spectral model was to quantify the major effect which is clearly seen in Fig. 1, namely the suppression of the reflection features in the energy spectrum with the increase of frequency.

The results of the analysis presented in this paper show that the relative amplitude of the reflected component variations is lower on the short time scales ( $\lesssim 50$ – $100$  msec), than that of the primary X-ray radiation. A similar effect was found by Oosterbroek et al. (1996) for GS 2023+338 but the characteristic time scale in this case was much longer,  $\sim 200$  sec. GS 2023+338 is peculiar in many ways. In particular the source exhibited strong ( $\gtrsim 10^{23}$  cm $^{-2}$ ) and highly variable (on the time scales of  $\sim 10^3$  sec) low energy absorption (e.g. Zycki et al., 1999) and, most importantly, extremely strong Fe line with equivalent width of up to 1.4 keV (Oosterbroek et al. 1996). That could mean that geometry of the reprocessing media in GS2023+338 is different from that in Cyg X-1. Recently we found the suppression of the reflected component variations in the low spectral state of another black hole candidate, GX339-4 (Revnivtsev, Gilfanov & Churazov, 1999). In this case the characteristic time scale ( $\sim 50$ – $100$  msec) was similar to that in Cyg X-1. We, therefore, can tentatively conclude that such behavior might be a common feature of the black hole binaries in the low spectral state.

A most straightforward explanation of this effect would be in terms of a finite light crossing time of the reflector  $\tau_{\text{refl}} \sim l_{\text{refl}}/c$ , caused by a finite spatial extend  $l_{\text{refl}}$  of the reflecting media. From Fig. 2 one can see that the equivalent width of the iron line drops by a factor of two at the frequency  $f_{1/2} \sim 10$  Hz. This value gives us a rough estimate of the characteristic response time of the reflector  $\tau_{\text{refl}} \sim 1/2\pi f_{1/2} \sim 15$  msec and the characteristic size of the reflecting media  $l_{\text{refl}} \sim 5 \times 10^8$  cm which would correspond to  $\sim 150R_g$  for a  $10M_\odot$  black hole. We note, however that if the primary continuum originates within the  $\sim 10R_g$  sphere in the inner zone of the accretion disk, then only a small fraction of the emitted hard radiation has the possibility to be reflected from the accretion disk regions with  $R \gtrsim 150R_g$  (in the case of a flat disk) and it can hardly provide the observed  $\sim 100$  eV equivalent width of the iron line. Therefore, the assumption that high frequency variations of the

reflected component are caused by the finite light crossing time of the reflector implies interesting constraints on the geometry of the source of the primary continuum and the reflector.

An alternative explanation might be that the short time scale,  $\lesssim 50\text{--}100$  msec, variations appear in the geometrically different, likely inner, part of the accretion flow and give a rise to significantly weaker, if any, reflected emission than the longer time scale events, presumably originating in the outer regions. This might be caused, for instance, by a smaller solid angle of the reflector as seen by the short time scale events and/or due to the screening of the reflector from the short time scale events by the outer parts of the accretion flow.

*Acknowledgements.* This research has made use of data obtained through the High Energy Astrophysics Science Archive Research Center Online Service, provided by the NASA/Goddard Space Flight Center.

## References

- Basko M., Sunyaev R. & Titarchuk L., 1974, *A&A*, 31, 249
- Ebisawa K., Inoue H., Mitsuda K., Nagase F., Tanaka Y., Yaqoob T., Yoshida K., 1992, in *Frontiers of X-ray Astronomy*, ed. Y. Tanaka & K. Koyama (Tokyo: University Press), 301
- George I.M., Fabian A.C., 1991, *MNRAS*, 249, 352
- Gierlinski M., Zdziarski A., Done C., Johnson W., Ebisawa K., Ueda Y., Haardt F., Philips B., 1997, *MNRAS*, 288, 958
- Miyamoto S., Kimura K., Kitamoto S., Dotani T., Ebisawa K., 1991, *ApJ*, 383, 784
- Nowak M., Vaughan B., Wilms J., Dove J., Begelman M., 1999, *ApJ*, 510, 874
- Oosterbroek T., van der Klis M., Vaughan B., van Paradijs J., Rutledge R., Lewin W.H.G., Tanaka Y., Nagase F., Dotani T., Mitsuda K., Yoshida K. 1996, *A&A*, 309, 781
- Revnivtsev M., Gilfanov M., Churazov E. 1999, in preparation
- Stark M., 1999, <http://lheawww.gsfc.nasa.gov/~stark/pca/pcabackest.html>
- Jahoda K., 1999, <http://lheawww.gsfc.nasa.gov/users/keith/pcarmf.html>
- Zycki P., Done C., Smith D. 1999, *MNRAS*, 305, 231